J. Fluid Mech. (1987), *vol.* 178, *pp.* 491–506
Printed in Great Britain

Rolls versus squares in thermal convection of fluids with temperature-dependent viscosity

By D. R. JENKINS†

Department of Applied Mathematics and Theoretical Physics, University of Cambridge, Silver Street, Cambridge CB3 9EW, UK

(Received 25 March 1986 and in revised form 8 October 1986)

We consider finite-amplitude thermal convection in a horizontal fluid layer. The viscosity of the fluid is dependent upon its temperature. Using a weakly nonlinear expansion procedure, we examine the stability of two-dimensional roll and three-dimensional square planforms, in order to determine which should be preferred in convection experiments. The analysis shows that the roll planform is preferred for low values of the ratio of the viscosities at the top and bottom boundaries, but the square planform is preferred for larger values of the ratio. At still larger values, subcritical convection is predicted. We also include the effects of boundaries having finite thermal conductivity, which enables favourable comparison to be made with experimental studies. A discrepancy between the present work and a previous study of this problem (Busse & Frick 1985) is discussed.

1. Introduction

There is much interest in thermal convection in fluids with temperature dependent viscosity, due mainly to its application to convection in the Earth's mantle. The mantle may be modelled as a fluid with strongly temperature-dependent viscosity, as it is known that the deformation of the mantle material is a strong function of temperature (Booker 1976; see also the reviews by Turcotte & Oxburgh 1972 and Peltier 1985). Also, observational evidence indicates that the planform of the convection is three-dimensional (McKenzie *et al.* 1980).

Several studies have been conducted into the effect of temperature dependence of viscosity upon the onset of convection in the Rayleigh–Bénard configuration. They include experiments (e.g. Hoard, Robertson & Acrivos 1970; Somerscales & Dougherty 1970) and theoretical studies (Booker 1976; Booker & Stengel 1978; Stengel, Oliver & Booker 1982). Stengel, Oliver & Booker have shown that the effect is dependent upon the form of the temperature dependence of the viscosity and the type of velocity boundary conditions used. For the case of viscosity varying exponentially with temperature they showed that the critical value of the Rayleigh number R (defined in terms of the viscosity at the midpoint of the layer) increases with the viscosity ratio r (defined as the ratio of viscosity at the top boundary to that at the bottom boundary) until $r \approx 1000$, and then rapidly decreases with r. Until R reaches its maximum value, the critical wavenumber varies very little, but then increases exponentially with r. Similar results have been found for super-exponential temperature dependence of viscosity, which is a realistic model for glycerol (Stengel *et al.* 1982), silicone oil (Oliver & Booker 1983) and golden syrup (White 1982).

† Present address: CSIRO Division of Mathematics and Statistics, PO Box 218, Lindfield, NSW 2070, Australia.

Theoretical planform studies have been primarily concerned with the effects of weak temperature dependence of viscosity. The analyses of Palm (1960), Segel & Stuart (1962), Palm & Oiann (1964) and Busse (1967) showed that the onset of convection occurs in the form of hexagons when r is small. Such behaviour is typical of convection in which the Boussinesq symmetry of the layer is broken. Busse (1967) also showed that the hexagonal planform is unstable to roll solutions if the Rayleigh number is increased slightly.

Experimental planform studies by Oliver (1980) and White (1982) both confirm the results of the weakly nonlinear analyses at low r, but the behaviour at higher r is quite different. Oliver's experiments (using silicone oil) show that hexagonal convection appears subcritically at large r. This planform eventually becomes unstable to a square planform if the Rayleigh number is sufficiently high (a few times critical). White's experiments (using golden syrup) were performed by inducing a particular planform at supercritical Rayleigh number and then slowly reducing R until convection no longer appeared. In this way White showed that both hexagonal and square planforms can be stable over a range of Rayleigh numbers including subcritical values, for r sufficiently large. In such a situation, initial conditions and the effects of sidewalls are likely to determine which planform is preferred.

Oliver & Booker (1983) proposed a weakly nonlinear analysis procedure to investigate the stability of square cells, but rejected its use because their experiments indicate that square cells are only stable at Rayleigh numbers significantly larger than critical. However, as White's experiments show that the square planform is stable near critical, a weakly nonlinear analysis can be useful. Busse & Frick (1985) (hereinafter called BF) consider a situation in which the viscosity of the fluid varies linearly with temperature, which is computationally convenient but not very realistic. They solve the Boussinesq equations for an infinite-Prandtl-number fluid by representing the velocity and temperature functions by low-order modal truncations. The stability of particular planforms is then determined by calculating the time evolution of the coefficients of each mode. The computational complexity of the solution procedure requires that the modal truncation be of low order and that only certain planforms be considered, so BF limit their analysis to roll and square planforms. Their results show that the square planform is stable provided r is sufficiently large. At small r, they find that the roll planform is the stable one. Near the critical Rayleigh number, they find that the changeover of stability from rolls to squares occurs at $r \approx 2$, and that as R is increased there is a range of r at which both rolls and squares are stable. They also find that neither square nor roll planforms exist subcritically over the range of r investigated.

In this paper we present a weakly nonlinear analysis of thermal convection with temperature-dependent viscosity, which is similar to that proposed by Oliver & Booker (1983). The problem is an extension of the analysis presented in Jenkins & Proctor (1984) (hereinafter called JP), which considered the effect of finite thermal conductivity of boundaries upon the convection planform.The analysis is presented in terms of a general temperature dependence of the fluid viscosity, and results are presented for a linear dependence, which allows comparison with the results of BF, and for an exponential dependence, which is closer to the behaviour of real fluids. The combined effects of temperature dependence of viscosity and finite conductivity boundaries are also investigated, enabling improved comparison with experimental studies.

2. Formulation

We consider a layer of Boussinesq fluid of depth d located between solid slabs of depth $\frac{1}{2}\lambda d$, where λ is of order unity. The thermal conductivity of the fluid is k and of the slabs is k_1; the respective thermal diffusivities are κ and κ_1 and ρ is the fluid density. All of k, k_1, κ and κ_1 are assumed to be constants. Cartesian coordinates are chosen with the origin at the midpoint of the layer. Gravity, $\boldsymbol{g}$ is perpendicular to the slabs; the fluid has velocity $\boldsymbol{u}$ and pressure p. The temperature T is fixed at the outer surfaces of the slabs, so that the overall temperature difference is ΔT. We let $\theta(\boldsymbol{x}, t)$ and $\tilde{\theta}(\boldsymbol{x}, t)$ represent temperature perturbations in the fluid and solid slabs respectively, from the basic state of no fluid motion and a conduction temperature profile. Then the equations of motion, heat and mass conservation in dimensionless form are

$$-\nabla p + R\theta\hat{\boldsymbol{z}} + \nabla\cdot\boldsymbol{S} = \frac{1}{\sigma}\left(\frac{\partial \boldsymbol{u}}{\partial t} + \boldsymbol{u}\cdot\nabla\boldsymbol{u}\right), \tag{2.1}$$

$$\boldsymbol{u}\cdot\hat{\boldsymbol{z}} + \nabla^2\theta = \frac{\partial\theta}{\partial t} + \boldsymbol{u}\cdot\nabla\theta, \tag{2.2}$$

$$\nabla\cdot\boldsymbol{u} = 0 \tag{2.3}$$

in the fluid and

$$\frac{\kappa_1}{\kappa}\nabla^2\tilde{\theta} = \frac{\partial\tilde{\theta}}{\partial t}$$

in the slabs. In (2.1), the tensor $\boldsymbol{S}$ is the stress tensor with

$$S_{ij} = \mu\left(\frac{\partial u_i}{\partial x_j} + \frac{\partial u_j}{\partial x_i}\right), \tag{2.4}$$

where μ is the dynamic viscosity of the fluid, made dimensionless by scaling with the viscosity at $z = 0(\mu_0)$. The dimensionless parameters are the Rayleigh number R and the Prandtl number σ, which are defined in terms of μ_0:

$$R = \frac{|\boldsymbol{g}|\,\alpha q d^4}{\kappa\nu_0}, \quad \sigma = \frac{\nu_0}{\kappa},$$

where $\nu_0 = \mu_0/\rho_0$ is the kinematic viscosity, ρ_0 is the fluid density at $z = 0$, q is the basic-state temperature gradient in the fluid and α is the coefficient of thermal expansion. Because fluids with significant temperature-dependent viscosity generally have high Prandtl number, we restrict the analysis by assuming infinite Prandtl number. Thus the right-hand side of (2.1) disappears. This assumption is consistent with most recent studies of convection with temperature-dependent viscosity.

The velocity vanishes on the boundary $z = \pm\frac{1}{2}$ and the temperature boundary conditions are

$$\tilde{\theta} = 0, \qquad z = \pm\tfrac{1}{2}(1+\lambda), \tag{2.5a}$$

$$\theta = \tilde{\theta}, \qquad z = \pm\tfrac{1}{2}, \tag{2.5b}$$

$$\mathrm{D}\theta = \zeta\mathrm{D}\tilde{\theta}, \quad z = \pm\tfrac{1}{2}, \tag{2.5c}$$

where $\zeta = k_1/k$ and D represents $\partial/\partial z$.

We represent the viscosity as a general function of the deviation from the reference temperature T_0

$$\mu = \mu(T - T_0). \tag{2.6}$$

Now in general we can write the velocity $\boldsymbol{u}$ as

$$\boldsymbol{u} = \boldsymbol{\nabla} \times \boldsymbol{\nabla} \times (\phi \hat{\boldsymbol{z}}) + \boldsymbol{\nabla} \times (\psi \hat{\boldsymbol{z}}). \tag{2.7}$$

In JP, the function ψ was zero because $\boldsymbol{u}$ was poloidal. BF point out that the nonlinearity introduced by the dependence of μ upon temperature is responsible for the generation of vertical vorticity, so ψ is non-zero. However, it is straightforward to show that the vertical vorticity is zero to the order required for the weakly nonlinear expansion considered here (see Oliver 1980). Hence we need not consider ψ.

3. Weakly nonlinear expansion

We expand $\boldsymbol{u}$, θ, $\tilde{\theta}$, p and R in powers of the small parameter ϵ as

$$\boldsymbol{u} = \epsilon \boldsymbol{u}_1 + \epsilon^2 \boldsymbol{u}_2 + \dots, \tag{3.1a}$$

$$\theta = \epsilon \theta_1 + \epsilon^2 \theta_2 + \dots, \tag{3.1b}$$

$$\tilde{\theta} = \epsilon \tilde{\theta}_1 + \epsilon^2 \tilde{\theta}_2 + \dots, \tag{3.1c}$$

$$p = \epsilon p_1 + \epsilon^2 p_2 + \dots, \tag{3.1d}$$

and

$$R = R_0 + \epsilon^2 R_2 + \dots, \tag{3.1e}$$

and scale the time t as

$$\frac{\partial}{\partial t} = \epsilon^2 \frac{\partial}{\partial \tau}. \tag{3.1f}$$

The expansions are the appropriate ones for the symmetries in the problem (see JP). Also, the viscosity must be expanded in terms of ϵ, because of its temperature dependence. Substituting the expansion

$$T - T_0 = -z + \epsilon \theta_1 + \epsilon^2 \theta_2 + \dots \tag{3.2}$$

into (2.6) yields, after some manipulation

$$\mu = U(z) - \epsilon \mathrm{D}U(z)\,\theta_1 + \epsilon^2 [\tfrac{1}{2}\mathrm{D}^2 U \theta_1^2 - \mathrm{D}U\theta_2] + O(\epsilon^3), \tag{3.3}$$

where

$$U(z) = \mu(-z)$$

and D represents d/dz. At leading order in ϵ, a linear time-independent problem is obtained, which can be reduced to

$$R_0 \nabla_{\mathrm{H}}^2 \theta_1 - \hat{\boldsymbol{z}} \cdot \boldsymbol{\nabla} \times \boldsymbol{\nabla} \times (\boldsymbol{\nabla} \cdot \boldsymbol{S}_1) = 0, \tag{3.4a}$$

$$w_1 + \nabla^2 \theta_1 = 0, \tag{3.4b}$$

$$\nabla^2 \tilde{\theta}_1 = 0, \tag{3.4c}$$

where ∇_{H}^2 is the horizontal Laplacian, w_1 is the vertical component of $\boldsymbol{u}_1$ and

$$S_{1ij} = U(z)\left(\frac{\partial u_{1i}}{\partial x_j} + \frac{\partial u_{1j}}{\partial x_i}\right). \tag{3.5}$$

Equation (3.4a) is obtained by operating on (2.1) with $\hat{\boldsymbol{z}} \cdot \boldsymbol{\nabla} \times \boldsymbol{\nabla} \times$. The boundary conditions on w_1 are

$$w_1 = \mathrm{D}w_1 \quad \text{on} \quad z = \pm \tfrac{1}{2} \tag{3.6}$$

and for θ_1 and $\tilde{\theta}_1$ are as given in conditions (2.5). The system (3.4) is separable in

the horizontal coordinates so we write $\phi_1 = f(x, y)\, h(z)$, $\theta_1 = f(x, y)\, g(z)$ and $\tilde{\theta}_1 = f(x, y)\, \tilde{g}(z)$, where f is the planform function, which satisfies

$$\nabla_{\mathrm{H}}^2 f = -a^2 f, \tag{3.7}$$

and substitute into (3.4) to yield

$$U(\mathrm{D}^2 - a^2)^2 h + 2\mathrm{D}U(\mathrm{D}^2 - a^2)\,\mathrm{D}h + \mathrm{D}^2 U(\mathrm{D}^2 + a^2)\, h = R_0 g, \tag{3.8a}$$

$$(\mathrm{D}^2 - a^2)\, g + a^2 h = 0, \tag{3.8b}$$

$$(\mathrm{D}^2 - a^2)\, \tilde{g} = 0, \tag{3.8c}$$

with boundary conditions

$$h = \mathrm{D}h = 0 \quad \text{on } z = \pm\tfrac{1}{2}, \tag{3.8d}$$

$$g = \tilde{g} \quad \text{on } z = \pm\tfrac{1}{2}, \tag{3.8e}$$

$$\mathrm{D}g = \zeta \mathrm{D}\tilde{g} \quad \text{on } z = \pm\tfrac{1}{2}, \tag{3.8f}$$

$$\tilde{g} = 0 \quad \text{on } z = \pm\tfrac{1}{2}(1+\lambda). \tag{3.8g}$$

If the viscosity function μ is a constant, which when scaled is unity, then (3.8) reduces to the linear eigenvalue problem considered by JP. Equations (3.8) may be solved numerically for any particular form of μ by discretizing the interval $-\frac{1}{2} \leqslant z \leqslant \frac{1}{2}$ and solving the resulting matrix eigenvalue problem by the inverse iteration method. This yields the critical Rayleigh number R_0 and corresponding wavenumber a as a function of λ and ζ. The linear problem has been solved by BF for a linear viscosity function and by Stengel *et al.* (1982) for an exponential viscosity function. Both studies assume that the boundaries of the fluid layer are perfect conductors of heat. The results of the present study match the previous results for both types of viscosity function, when ζ is set to a sufficiently large value. At second order in ϵ the following system arises:

$$R_0 \nabla_{\mathrm{H}}^2 \theta_2 - \hat{\boldsymbol{z}} \cdot \boldsymbol{\nabla} \times \boldsymbol{\nabla} \times (\boldsymbol{\nabla} \cdot \boldsymbol{S}_2^{(\ell)}) = \hat{\boldsymbol{z}} \cdot \boldsymbol{\nabla} \times \boldsymbol{\nabla} \times (\boldsymbol{\nabla} \cdot \boldsymbol{S}_2^{(\mathrm{n})}), \tag{3.9a}$$

$$w_2 + \nabla^2 \theta_2 = \boldsymbol{u}_1 \cdot \boldsymbol{\nabla} \theta_1, \tag{3.9b}$$

$$\nabla^2 \tilde{\theta}_2 = 0, \tag{3.9c}$$

where

$$S_{2ij}^{(\ell)} = U\left(\frac{\partial u_{2i}}{\partial x_j} + \frac{\partial u_{2j}}{\partial x_i}\right), \tag{3.10a}$$

$$S_{2ij}^{(\mathrm{n})} = -\theta_1 \mathrm{D}U\left(\frac{\partial u_{1i}}{\partial x_j} + \frac{\partial u_{1j}}{\partial x_i}\right). \tag{3.10b}$$

Note that $\boldsymbol{S}_2^{(\ell)}$ is linear in $\boldsymbol{u}_2$ while $\boldsymbol{S}_2^{(\mathrm{n})}$ is nonlinear in the first-order eigenfunctions. The boundary conditions for $\boldsymbol{u}_2$, θ_2 and $\tilde{\theta}_2$ are identical with those for $\boldsymbol{u}_1$, θ_1 and $\tilde{\theta}_1$, respectively. We assume that the planform function f takes the form

$$f = A(\tau) \cos ax + B(\tau) \cos ay, \tag{3.11}$$

which can represent both roll and square planforms, and then evaluate the right-hand sides of (3.9). This results in a set of inhomogeneous linear ordinary differential equations for the vertical dependences of each of the horizontal modes arising from the form of the right-hand sides, which are solved numerically on the same finite-difference grid as the linear equations.

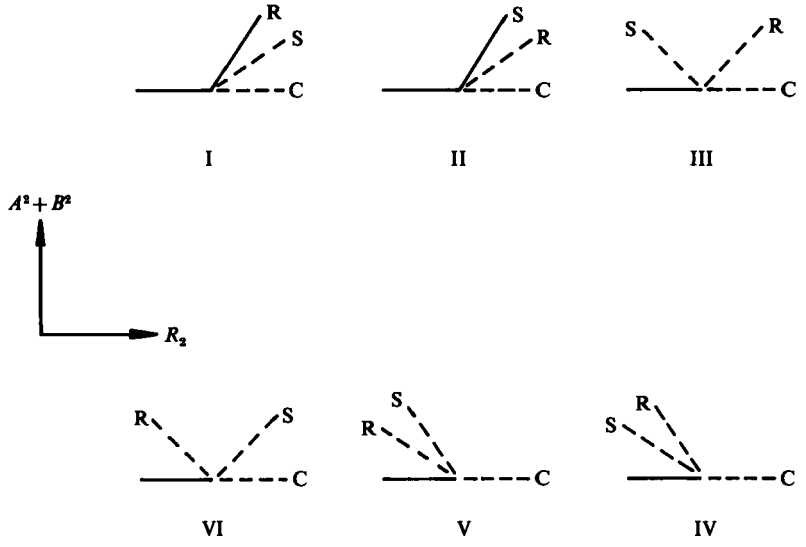

FIGURE 1. Bifurcation diagrams for the steady states of (3.15). The six different situations correspond to the conditions on the coefficients E and F given in Table 1. Dashed lines represent unstable states and solid lines represent stable states. $C \equiv$ conduction; $R \equiv$ roll; $S \equiv$ square. Adapted from Swift (1984).

Finally, at third order in the expansion, the system of equations

$$-\nabla p_3 + R_0\theta_3\hat{\boldsymbol{z}} + \nabla\cdot\boldsymbol{S}_3^{(\ell)} = -\nabla\cdot\boldsymbol{S}_3^{(\mathrm{n})} - R_2\theta_1\hat{\boldsymbol{z}}, \tag{3.12a}$$

$$w_3 + \nabla^2\theta_3 = \frac{\partial\theta_1}{\partial\tau} + \boldsymbol{u}_1\cdot\nabla\theta_2 + \boldsymbol{u}_2\cdot\nabla\theta_1, \tag{3.12b}$$

$$\nabla\cdot\boldsymbol{u}_3 = 0, \tag{3.12c}$$

$$\nabla^2\tilde{\theta}_3 = \frac{\kappa}{\kappa_1}\frac{\partial\tilde{\theta}_1}{\partial\tau}, \tag{3.12d}$$

where

$$S_{3ij}^{(\ell)} = U\left(\frac{\partial u_{3i}}{\partial x_j} + \frac{\partial u_{3j}}{\partial x_i}\right), \tag{3.13a}$$

$$S_{3ij}^{(\mathrm{n})} = -\theta_1\,\mathrm{D}U\left(\frac{\partial u_{2i}}{\partial x_j} + \frac{\partial u_{2j}}{\partial x_i}\right) - (\theta_2\,\mathrm{D}U - \tfrac{1}{2}\theta_1^2\,\mathrm{D}^2U)\left(\frac{\partial u_{1i}}{\partial x_j} + \frac{\partial u_{1j}}{\partial x_i}\right). \tag{3.13b}$$

Note that $\boldsymbol{S}_3^{(\ell)}$ is linear in $\boldsymbol{u}_3$, and so has been included in the homogeneous part of (3.12a), while $\boldsymbol{S}_3^{(\mathrm{n})}$ is nonlinear in the lower-order functions. The boundary conditions for $\boldsymbol{u}_3$, θ_3 and $\tilde{\theta}_3$ are identical with those for $\boldsymbol{u}_1$, θ_1 and $\tilde{\theta}_1$, respectively. We determine a solvability condition for this inhomogeneous linear boundary-value problem, which must be satisfied for all $\boldsymbol{u}^*$, θ^* and $\tilde{\theta}^*$ that are solutions of the homogeneous adjoint problem. In this case the solvability condition is

$$R_0\left\langle\theta^*\left[\frac{\partial\theta_1}{\partial\tau} + \boldsymbol{u}_1\cdot\nabla\theta_2 + \boldsymbol{u}_2\cdot\nabla\theta_1\right]\right\rangle - R_2\langle w^*\theta_1\rangle - \langle\boldsymbol{u}^*\cdot\nabla\cdot\boldsymbol{S}_3^{(\mathrm{n})}\rangle - R_0\zeta\frac{\kappa}{\kappa_1}\left\{\tilde{\theta}^*\frac{\partial\tilde{\theta}_1}{\partial\tau}\right\} = 0, \tag{3.14}$$

I	$E-F>0$	$E+F<0$	$E<0$	stable supercritical rolls
II	$E-F<0$	$E+F<0$	$E<0$	stable supercritical squares
III	$E-F<0$	$E+F>0$	$E<0$	subcritical squares
IV	$E-F<0$	$E+F>0$	$E>0$	subcritical rolls and squares
V	$E-F>0$	$E+F>0$	$E>0$	subcritical rolls and squares
VI	$E-F>0$	$E+F<0$	$E>0$	subcritical rolls

TABLE 1. Steady states of (3.15)

where the angled brackets denote averaging over the fluid layer and the braces denote averaging over the slabs. The homogeneous part of the boundary-value problem consisting of (3.12) and its boundary conditions is the same as the first-order problem, which is self-adjoint for the inner product represented by the averaging, so $\boldsymbol{u}^*$, θ^* and $\tilde{\theta}^*$ are the first-order solutions. Evaluation of (3.14) for each of the horizontal modes in (3.11) leads to the following time-evolution equations for the amplitudes A and B:

$$\frac{\mathrm{d}A}{\mathrm{d}\tau} = R_2 A + EA^3 + FAB^2, \tag{3.15a}$$

$$\frac{\mathrm{d}B}{\mathrm{d}\tau} = R_2 B + EB^3 + FA^2 B. \tag{3.15b}$$

The coefficients E and F are integrations over the vertical coordinate of expressions involving the linear functions evaluated at first and second order.

The steady-solutions of (3.15) are the conduction state ($A = B = 0$), the roll planform (one of A or B zero) and the square planform ($A^2 = B^2 \neq 0$). Swift (1984), in a comprehensive study of convective planform selection, has identified six possible sets of behaviour for solutions of (3.15), depending upon the sign and magnitude of the coefficients E and F. In fact, there are three relevant combinations of E and F that determine the behaviour: $E-F$, $E+F$ and E. Figure 1 shows bifurcation diagrams for the six different cases that exist under the conditions given in table 1. These can be determined by considering the linear stability of each of the steady states. In the next section we evaluate E and F as functions of r for linear and exponential viscosity functions and determine which of the states in figure 1 is appropriate.

4. Results

We consider two types of viscosity function:

$$\mu(T-T_0) = 1-\eta(T-T_0), \tag{4.1a}$$

$$\mu(T-T_0) = \mathrm{e}^{-\eta(T-T_0)}. \tag{4.1b}$$

The most useful parameter for comparison between different forms of μ and also for comparison with other research is the viscosity ratio r, which is defined as

$$r = \frac{\mu_{\max}}{\mu_{\min}}, \tag{4.2}$$

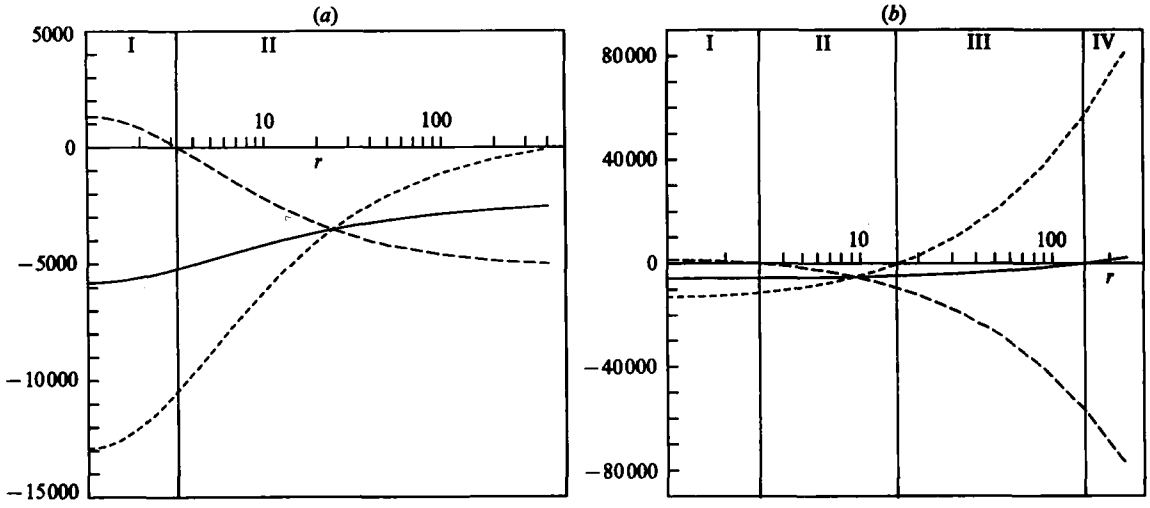

FIGURE 2. Graphs of the coefficient combinations E (solid line), $E-F$ (dashed) and $E+F$ (short dashed) as functions of the viscosity ratio r, with $\zeta = \infty$ and $\lambda = 1$, for (*a*) a *linear* viscosity function (equation (4.1*a*)) and (*b*) an *exponential* viscosity function (equation (4.1*b*)). The Roman numerals correspond to the steady states in table 1.

where $\mu_{\max}$ and $\mu_{\min}$ are the viscosities at the top and bottom of the layer, respectively. The relationships between r and the parameter η for the two functions given in (4.1) are

$$r = \frac{2+\eta}{2-\eta}, \tag{4.3a}$$

$$r = \mathrm{e}^{\eta}. \tag{4.3b}$$

The linear function has been investigated by BF and so provides a basis for comparison with the results derived here. The exponential function has been investigated by Stengel *et al.* (1982) for its effect upon the linear stability of convection and some initial work has been done by Oliver (1980) to investigate the stable planforms. The exponential function is a more realistic form for the temperature dependence of viscosity, particularly as η (and hence r) becomes large. Note that the linear function has a limiting value of $\eta = 2$ at which the viscosity ratio becomes infinite.

4.1. *Perfectly conducting boundaries*

The limiting case of $\zeta \to \infty$ is approximated by setting ζ to an extremely large value for the numerical evaluation of the coefficients, which is justified because the problem is well behaved in this limit. In figure 2 we show graphs of $E-F$, $E+F$ and E as functions of the viscosity ratio r, for the linear and exponential functions. The important points on the graphs are the intercept of each curve with the horizontal axis. Each intercept indicates a change in behaviour as given by figure 1 and table 1. We call the $(E-F)$-intercept r_1, the $(E+F)$-intercept r_2 and the E-intercept r_3. Figure 2(*a*) shows that only types I and II of table 1 exist, at least up to $r = 399$, so convection always occurs supercritically in this range. It is not clear whether the curve of $E+F$ asymptotes to the horizontal axis, always remaining negative, or

it crosses the axis at larger r. The accuracy of the solution procedure for $r > 399$ is not sufficiently high to be able to resolve this point. However, the results are a considerable advance on those of BF, who only examined the problem for values of r up to order 10, albeit for a larger range of Rayleigh number than applicable here. Note that $r = 399$ corresponds to $\eta = 1.99$, which is approaching the limit $\eta = 2$ at which r becomes infinite. A more sophisticated solution procedure would be required for accurate determination of the behaviour in this limit, but it is questionable whether the effort required is of much use, since the limit does not correspond to any realistic behaviour. With the exponential viscosity function, the above problem does not arise.

The other feature to notice from figure 2(*a*) is that the stable planform changes from rolls at low values of r to squares at higher r. The changeover occurs at $r_1 \approx 3.2$. This value is different to that calculated by BF using a different method. They find that $r_1 \approx 2$. It is not clear why there should be such a difference. The algebra required to calculate E and F has been carefully checked, as has the computer code that is used to evaluate them. The lack of agreement with the work of BF means that other forms of verification are required. We show in the following section that the calculations presented here agree with the behaviour determined for the limit of almost insulating boundaries by Gertsberg & Sivashinsky (1981), thus providing some evidence for the accuracy of the present results.

The results shown in figure 2(*b*) are significantly different from those in figure 2(*a*) and provide new information about thermal convection with temperature-dependent viscosity. The figure shows that all of the states I, II, III and IV exist as r is increased. As in the linear case, the roll planform is stable until $r = r_1 \approx 3$ and then the square planform is stable, and convection is supercritical. However, when $r = r_2 (\approx 16)$, $E+F$ changes sign, so square-planform convection can occur subcritically, and when $r = r_3 (\approx 145)$, E changes sign, whence both rolls and squares can exist subcritically. The existence of subcritical square-planform convection is a significant new result.

4.2. *Finite-conductivity boundaries*

As examples of the effect of finite-conductivity boundaries upon the results given above, the graphs of figures 3 and 4 are presented. Figure 3 plots the curves of $E-F$, $E+F$ and E as functions of r for the exponential viscosity function, with the boundary conditions modified so that $\zeta = 10$ and $\lambda = 1$. The value of $\zeta = 10$ has been chosen because it is comparable with the value of ζ used in experiments with transparent boundaries (e.g. Le Gal, Pocheau & Croquette 1985, have $\zeta = 7$ for glass boundaries with silicone oil as the fluid) and also because it is above the value of ζ for which the changeover from rolls to squares occurs (ζ_c) when the viscosity is a constant (JP show $\zeta_c \approx 1$ for high-Prandtl-number fluids, with $\lambda = 1$). The values of r_1, r_2 and r_3 in this case are less than those for the perfectly conducting case. Here, $r_1 \approx 2.5$ (3), $r_2 \approx 13$ (16) and $r_3 \approx 140$ (145). The figures in brackets are the values for $\zeta = \infty$. Figure 4 shows graphs of $E-F$, $E+F$ and E for both linear and exponential viscosity functions, with $\zeta = 0.1$ and $\lambda = 1$. In this case $\zeta < \zeta_c$ for the constant-viscosity case. Thus the $E-F$ curve is always negative, so stable supercritical rolls (state I in table 1) cannot exist. Figure 4(*a*) shows that $r_2 \approx 2.2$ and $r_3 \approx 9$ for the linear function, which means that subcritical convection can occur with a linear viscosity variation. Figure 4(*b*) shows that $r_2 \approx 2$ and $r_3 \approx 13$ for the exponential function. It is clear that for low r, and thus low η, the linear viscosity function approximates the exponential one. Thus it is to be expected that the behaviour of the convection in

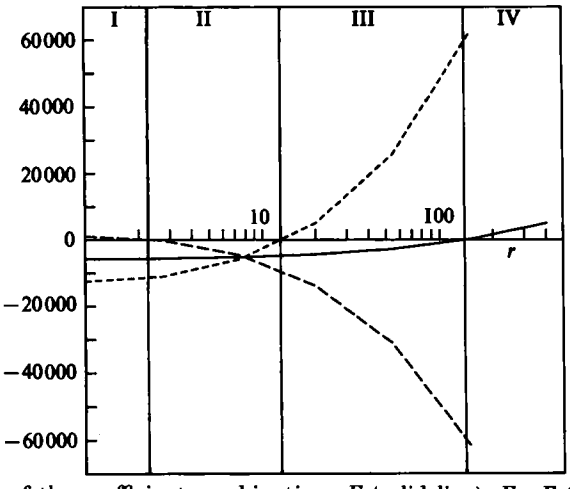

FIGURE 3. Graph of the coefficient combinations E (solid line), $E-F$ (dashed) and $E+F$ (short dashed) as functions of the viscosity ratio r, with $\zeta = 10$ and $\lambda = 1$ for an exponential viscosity function (equation (4.1b)).

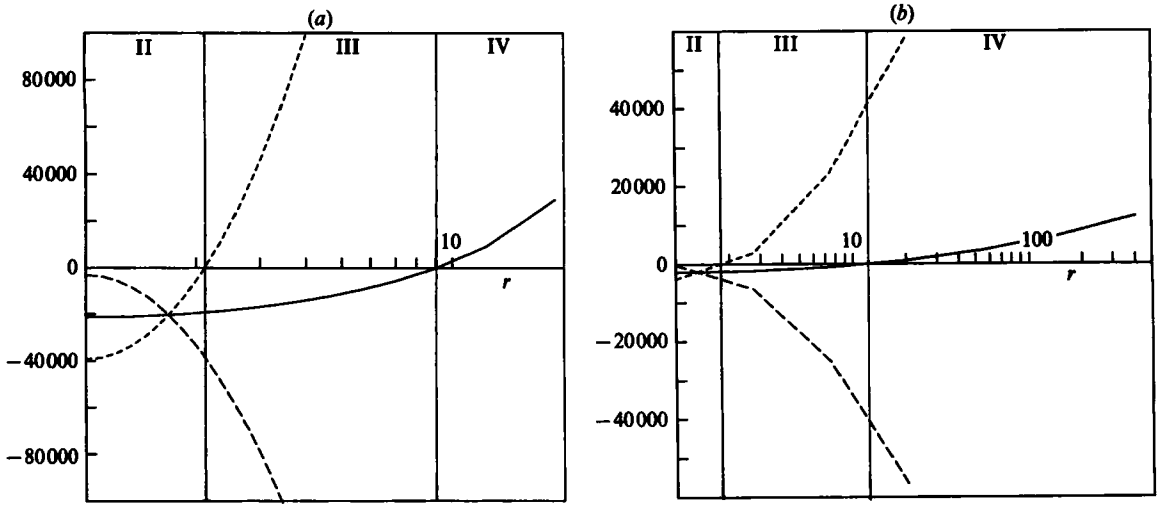

FIGURE 4. Graphs of the coefficient combinations E (solid line), $E-F$ (dashed) and $E+F$ (short dashed) as functions of the viscosity ratio r, with $\zeta = 0.1$ and $\lambda = 1$ for (a) a linear viscosity function (equation (4.1a)) and (b) an exponential viscosity function (equation (4.1b)).

these two cases should be similar at low η, and indeed it is. The effect of the low-conductivity boundaries is to emphasize the similarity of behaviour.

4.3. *Comparison with experiments*

The experiments of White (1982) used Golden Syrup as the working fluid and Perspex boundaries. Appropriate parameter values for this configuration are $\lambda = 0.25$ and $\zeta = 3$. Using these values, we have calculated E and F for various r and found that a square planform is stable for $r > 2.4$ and a subcritical square planform is possible for $r > 13$. This is to be compared with White's claim that he observed subcritical squares for $r > 6$.

The appropriate parameter values for the experiments of Le Gal *et al.* (1985) are $\lambda = 6$ and $\zeta = 7$. With silicone oil as the working fluid, the viscosity ratio they used was $r = 1.12$. Using these values, we find that

$$E - F = 429,$$

$$E + F = -8341,$$

$$E = -3956,$$

which means that $r < r_1$ (type I behaviour) indicating that rolls, rather than squares, are stable. Le Gal *et al.* observed a stable square planform for slightly supercritical Rayleigh numbers.

The reasons for the discrepancies between two sets of carefully controlled experiments and the present theory are not clear. There is good qualitative agreement with White's results, but differences may be due to the type of viscosity function used and also to errors in estimating the critical Rayleigh number by White due to the finite thermal conductivity of the boundaries. The effect of sidewalls in experiments may also be important. Bernoff (1985) has considered the effects of sidewalls upon the stability of the square planform in a container having the symmetry of a square and has shown that it is always stable for $R - R_0$ sufficiently small, even when the top and bottom boundaries are perfect conductors of heat and the fluid viscosity is independent of temperature. However, it rapidly loses stability as $R - R_0$ is increased. Although the experiments of Le Gal *et al.* used a circular container, the results of Bernoff's analysis provide evidence that the sidewalls may be extremely significant.

5. Almost insulating boundaries

Gertsberg & Sivashinsky (1981) and Depassier & Spiegel (1982) have considered the problem of thermal convection between almost insulating boundaries, including the effect of a weak temperature dependence of the fluid viscosity. In the insulating limit, the wavenumber of the convection becomes small, and an expansion scheme can be developed which separates the vertical and horizontal coordinates. Gertsberg & Sivashinsky presented a similar analysis to Chapman & Proctor (1980) and Proctor (1981) and developed almost identical equations for the horizontal dependence of convection. However, including the effects of temperature-dependent viscosity into the analysis adds an extra term to the equation. They consider a viscosity variation of the form

$$\mu(T - T_0) = 1 - \epsilon^2 \xi (T - T_0), \tag{5.1}$$

where $\epsilon = O(\zeta^{\frac{1}{4}})$ and ξ is $O(1)$. Although Gertsberg & Sivashinsky do not include the temperature-dependent viscosity term in their analysis of three-dimensional convection, it is possible to infer its form from the two-dimensional equation. The appropriate equation for the planform function f is then

$$f_t = -A(R - R_c)\nabla_H^2 f - B\nabla_H^4 f + C\nabla_H \cdot (|\nabla_H f|^2 \nabla_H f) + \xi \nabla_H \cdot (f \nabla_H f) + \mathrm{D}\theta|_{z=\frac{1}{2}}, \tag{5.2}$$

where the constants A, B, C and R_c are (for rigid boundaries)

$$A = \tfrac{1}{720}, \quad B = \tfrac{17}{462}, \quad C = \tfrac{10}{7}, \quad R_c = 720.$$

An appropriate expansion procedure can be applied to (5.2) in order to derive

	Asymptotic		Calculated	
$\eta \times 10^3$	E	F	E	F
0	−1.272	−0.8478	−1.258	−0.8390
0.5	−1.107	2.1195	−1.108	2.0723
1.0	−0.6123	11.02	−0.6111	10.88
1.5	0.2120	25.85	0.2195	25.65

TABLE 2. Asymptotic comparison. Calculations used $\zeta = 10^{-7}$.

evolution equations for comparison with the computational work described in the previous sections. The coefficients of the evolution equations then turn out to be

$$E = \frac{\eta^2}{18A\zeta^{\frac{1}{2}}B^{\frac{1}{2}}} - \frac{3C\zeta^{\frac{1}{2}}}{4AB^{\frac{1}{2}}}, \tag{5.3}$$

$$F = \frac{\eta^2}{A\zeta^{\frac{1}{2}}B^{\frac{1}{2}}} - \frac{C\zeta^{\frac{1}{2}}}{2AB^{\frac{1}{2}}}, \tag{5.4}$$

where $\eta = \zeta^{\frac{1}{2}}\xi$ is the viscosity-variation parameter used in the previous sections. The above expressions for E and F can be compared with the computed values at low ζ and η as a check on the procedure employed here. Table 2 shows such a comparison for the case $\zeta = 10^{-7}$ and various η. It is evident from the table that the computed coefficients approximate the asymptotic behaviour given by (5.3) and (5.4).

6. Degenerate points

The points where $E-F$, $E+F$ and E change sign (r_1, r_2 and r_3 respectively) are points of degeneracy. In the neighbourhood of these points the above analysis cannot determine the stable planform, so a higher-order analysis is required. It is necessary to expand about the degenerate point in terms of both R and r. The evolution equations necessary for describing the stable solutions require terms up to fifth order in amplitude. The results of BF illustrate the type of behaviour near the degenerate point r_1 ($E-F=0$). They found that both squares and rolls are stable over a range of r-values near r_1 for supercritical Rayleigh numbers. The relevant amplitude equation in this case is (adapted from Swift 1984)

$$\frac{\mathrm{d}A}{\mathrm{d}\tau} = A[R_2 + E(A^2+B^2) + \delta B^2 + G(A^2+B^2)^2 + HA^4 + KB^4], \tag{6.1}$$

where δ is a small parameter representing the deviation from the degenerate point and G, H and K are $O(1)$ coefficients. The equation for the evolution of B takes the same form, with A and B interchanged. Swift showed that for the case $E < 0$, there are two possible types of behaviour depending on the sign of $H+K$, as illustrated by the bifurcation diagrams of figure 5. The results of BF show that in the region marked III in figure 5 both squares and rolls are stable, indicating that in this problem $H+K > 0$. The similarity of the bifurcation diagram of figure 5 to the results of BF indicates the amount of information that can be derived from a weakly nonlinear analysis provided that the expansion is carried to sufficiently high orders. The problem with including the higher-order terms is the large amount of algebra and computing required to evaluate the coefficients.

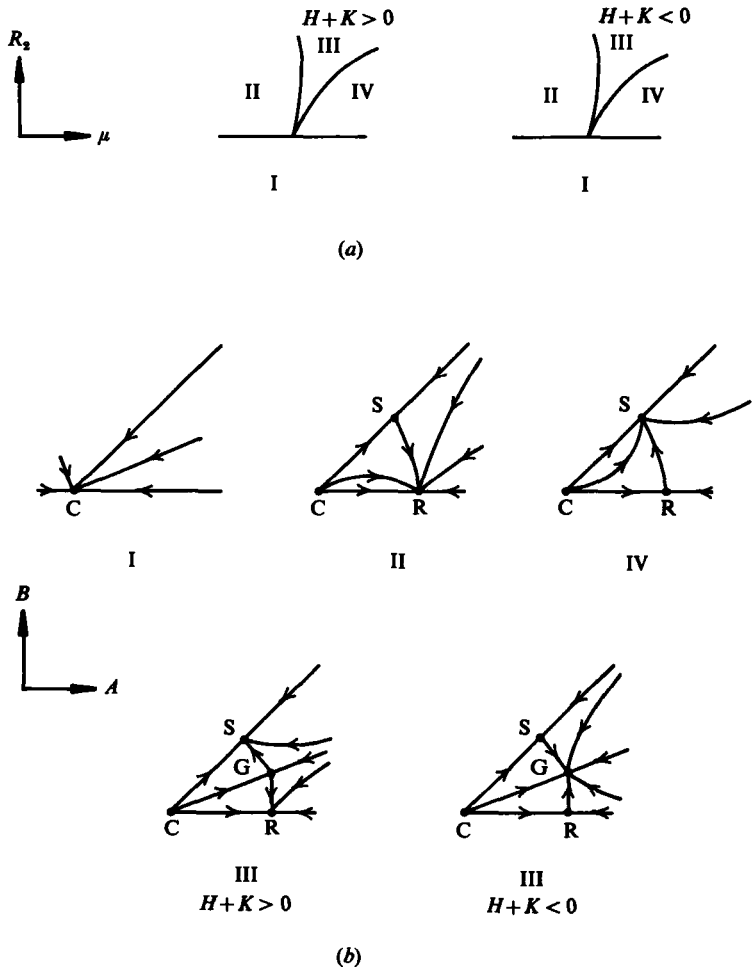

FIGURE 5. (*a*) Bifurcation diagrams and (*b*) phase portraits for the steady states of equation (6.1). The state G is a general solution, whose stability depends upon the sign of $H+K$. $C \equiv$ conduction; $R \equiv$ roll; $S \equiv$ square. Adapted from Swift (1984).

It is possible to carry the expansion procedure to fifth order in the limit of $\zeta \to 0$. The algebra involved in expanding the Gertsberg–Sivashinsky equation is less tedious than expanding the full problem at finite ζ. There are only two degenerate points in this limit. The combination $E-F$ is always negative, because the poorly conducting boundaries stabilize the square-cell planform. But we see from (5.3) and (5.4) that

$$E+F=0 \quad \text{when } \eta^2 = \tfrac{45}{38}C\zeta,$$

$$E=0 \quad \text{when } \eta^2 = \tfrac{27}{2}C\zeta.$$

Gertsberg & Sivashinsky (1981) have considered the degeneracy $E=0$, since the behaviour depends only upon the sign of the A^5 coefficient in the amplitude equation, which can be determined from their two-dimensional analysis. The relevant fifth-order amplitude equation is (Swift 1984)

$$\frac{\mathrm{d}A}{\mathrm{d}\tau} = A[R_2 + FB^2 + \delta(A^2+B^2) + HA^4]. \tag{6.2}$$

Swift showed that when $E-F<0$, which is the case when $E=0$ in this problem, all steady solutions of (6.2) are unstable, so that very little extra information about the nature of the planform near r_3 has been obtained from the fifth-order calculation.

For the degenerate point r_2 at which $E+F=0$, the relevant fifth-order amplitude equation is (Swift 1984)

$$\frac{\mathrm{d}A}{\mathrm{d}\tau} = A[R_2+2FB^2+\delta(A^2+B^2)+GA^2B^2+HA^4+KB^4] \tag{6.3}$$

and the behaviour depends upon the sign of $G+H+K$. This case is interesting because a stable subcritical square planform exists provided $G+H+K<0$. Hence the possibility of observing such a planform in experiments has a theoretical basis.

7. Discussion

The present study has provided significant insight into the stability of the square planform when the viscosity of the fluid in a Rayleigh–Bénard configuration is dependent upon temperature. Prior to this, the only theoretical study of the problem was by Busse & Frick (1985), but the viscosity function they used is unrealistic and causes computational problems as the ratio r of viscosities at the top and bottom of the layer becomes large. Here we have shown that the results of BF are limited by the small range of r that they studied. The present work extends their analysis to higher values of r, although it is valid only near the onset of convection. The results indicate that subcritical square-cell convection may occur for r sufficiently large, when the boundaries of the fluid layer are perfect conductors of heat. Although it was not possible to show this explicitly, owing to the singular nature of the viscosity function, it could be inferred from the results at lower values of r and the results when the boundaries are poor conductors of heat. Thus we have shown results that are qualitatively similar to those of BF, but some numerical discrepancies exist. The analysis in the limit of almost insulating boundaries given above serves to substantiate the numerical results in the present study.

Because the analysis presented here is developed for a general functional dependence of viscosity, it has been possible to produce results for a more realistic temperature dependence than that studied by BF. The exponential profile has been chosen for its similarity to the actual dependence of many fluids. Also it does not exhibit singular behaviour as r becomes large, so computation is less difficult than with the linear function. The drawback is that the expressions required to evaluate the coefficients of the evolution equations are much longer. Oliver (1980) carried out a similar analysis to the one given here for an exponential viscosity function, but only performed the relevant calculations up to second order. We have completed the calculations proposed by Oliver and then extended the analysis by considering the possibility of boundaries with finite thermal conductivity.

Finally, we have compared the analysis with experimental studies of square-planform convection for fluids with temperature-dependent viscosity. We found qualitative agreement with the results of White (1982), but quantitative differences still exist between theory and experiment, possibly due to the presence of sidewalls in the experiments.

The comparison of square-planform convection as discussed in this paper with

experimental observations of square-cell convection is clouded by the question of the validity of the expression

$$f = \cos ax + \cos ay \tag{7.1}$$

as a prototype form for square convection. Stuart (1964) proposed that the above representation is not valid, because there is no unambiguous means of determining cellular boundaries, defined as surfaces through which no fluid passes. However, there is no doubt that square-cell convection has been observed e.g. by White (1982), Oliver & Booker (1983) and Le Gal *et al.* (1985). We believe that square-planform convection as represented by (7.1) does produce patterns similar to those obtained in experiments, when the effects of the shadowgraph technique are considered. This technique, which relies upon the variation of the refractive index of the convecting fluid with its density, and hence temperature, is a commonly used means of observing convection planforms. Recent work (Jenkins 1987) shows that the shadowgraph pattern of (7.1) results in unambiguous square cellular boundaries that represent surfaces through which no fluid passes. The pattern closely resembles some observed shadowgraph patterns of square cells.

The author gratefully acknowledges many hours of helpful discussion on this problem from M. R. E. Proctor and A. J. Bernoff. The work presented in this paper was done during my Ph.D. studies in Cambridge. Financial support during this time was provided under the Commonwealth Scholarship and Fellowship Plan.

REFERENCES

Bernoff, A. J. 1985 Sidewall stabilisation of convection. Preprint, University of Cambridge.

Booker, J. R. 1976 Thermal convection with strongly temperature-dependent viscosity. *J. Fluid Mech.* **76**, 741–754.

Booker, J. R. & Stengel, K. C. 1978 Further thoughts on convective heat transport in a variable-viscosity fluid. *J. Fluid Mech.* **86**, 289–291.

Busse, F. H. 1967 The stability of finite amplitude cellular convection and its relation to an extremum principle. *J. Fluid Mech.* **30**, 625–629.

Busse, F. H. & Frick, H. 1985 Square-pattern convection in fluids with strongly temperature-dependent viscosity. *J. Fluid Mech.* **150**, 451–465.

Chapman, C. J. & Proctor, M. R. E. 1980 Nonlinear Rayleigh–Bénard convection between poorly conducting boundaries. *J. Fluid Mech.* **101**, 759–782.

Depassier, M. C. & Spiegel, E. A. 1982 Convection with heat flux prescribed on the boundaries of the system. I. The effect of temperature dependence of material properties. *Geophys. Astrophys. Fluid Dyn.* **21**, 167–188.

Gertsberg, V. L. & Sivashinsky, G. I. 1981 Large cells in nonlinear Rayleigh–Bénard convection. *Prog. Theor. Phys.* **66**, 1219–1229.

Hoard, C. Q., Robertson, C. R. & Acrivos, A. 1970 Experiments on the cellular structure in Bénard convection. *Intl J. Heat Mass Transfer* **13**, 849–855.

Jenkins, D. R. & Proctor, M. R. E. 1984 The transition from roll to square-cell solutions in Rayleigh–Bénard convection. *J. Fluid Mech.* **139**, 461–471.

Jenkins, D. R. 1987 Interpretation of shadowgraph patterns in Rayleigh–Bénard convection, *J. Fluid Mech.* (submitted).

Le Gal, P., Pocheau, A. & Croquette, V. 1985 Square versus roll pattern at convective threshold. *Phys. Rev. Lett.* **54**, 2501–2504.

McKenzie, D., Watts, A., Parsons, B. & Roufosse, M. 1980 Planform of mantle convection beneath the Pacific Ocean. *Nature* **288**, 422–445.

OLIVER, D. S. 1980 Bénard convection with strongly temperature dependent viscosity. Ph.D. thesis, University of Washington.

OLIVER, D. S. & BOOKER, J. R. 1983 Planform of convection with strongly temperature dependent viscosity. *Geophys. Astrophys. Fluid Dyn.* **27**, 73–85.

PALM, E. 1960 On the tendency towards hexagonal cells in steady convection. *J. Fluid Mech.* **8**, 183–192.

PALM, E. & OIANN, H. 1964 Contribution to the theory of cellular thermal convection. *J. Fluid Mech.* **19**, 353–365.

PELTIER, W. R. 1985 Mantle convection and viscoelasticity. *Ann. Rev. Fluid Mech.* **17**, 561–608.

PROCTOR, M. R. E. 1981 Planform selection by finite-amplitude thermal convection between poorly conducting slabs. *J. Fluid Mech.* **113**, 469–485.

SEGEL L. A. & STUART, J. T. 1962 On the question of the preferred mode in cellular thermal convection. *J. Fluid Mech.* **13**, 289–306.

SOMERSCALES, E. F. C. & DOUGHERTY T. S. 1970 Observed flow patterns at the initiation of convection in a horizontal liquid layer heated from below. *J. Fluid Mech.* **42**, 755–768.

STENGEL, K. C., OLIVER, D. S. & BOOKER, J. R. 1982 Onset of convection in a variable-viscosity fluid. *J. Fluid Mech.* **120**, 411–431.

STUART, J. T. 1964 On the cellular patterns in thermal convection. *J. Fluid Mech.* **18**, 481–496.

SWIFT, J. W. 1984 Bifurcation and symmetry in convection. Ph.D. dissertation, University of California, Berkeley.

TURCOTTE, D. L. & OXBURGH, E. R. 1972 Mantle convection and the new global tectonics. *Ann. Rev. Fluid Mech.* **4**, 33–68.

WHITE, D. B. 1982 Experiments with convection in a variable viscosity fluid. Ph.D. thesis, University of Cambridge.